

Consistent microscopic study of the low-energy ${}^5\text{Li}$ spectrum

Gerd Blüge and Karlheinz Langanke

Institut für Theoretische Physik I, Universität Münster, D-4400 Münster, West Germany

(Received 28 August 1989)

We have studied the nucleus ${}^5\text{Li}$ within a multichannel resonating group calculation based on many-body $p + \alpha$ and $d + {}^3\text{He}$ configurations and pseudostates as well as on effective nucleon-nucleon interactions containing central, spin-orbit, and tensor components. The known levels in ${}^5\text{Li}$, identified by the $p + \alpha$ phase shifts and the ${}^3\text{He}(d,p){}^4\text{He}$ fusion cross section, can consistently be described by our approach. Special distortion effects in the sense of Tang and collaborators are discussed for these states.

I. INTRODUCTION

The consideration of specific distortion effects has been shown to be important in studies of nuclear reactions based on the framework of microscopic cluster models.^{1,2} Being dependent on the compressibility of the respective nuclear fragment, these distortion effects are especially important in reactions involving a deuteron. For example, in studying the $d + {}^3\text{He}$ system, Tang and collaborators obtained reasonable results in the $d + {}^3\text{He}$ channel with channel spin $S = \frac{1}{2}$ via the consideration of a $p + \alpha$ configuration, while in the $S = \frac{3}{2}$ channel these effects have been simulated by introducing cluster pseudostates.^{3,4} The authors stressed the nice feature that they were able to simultaneously describe both channels with the same (central) nucleon-nucleon (NN) interaction which they had adjusted to the empirical p -wave phase shifts in the $n + \alpha$ system. Despite the important improvement which could be achieved by considering specific distortion effects, the calculation of Shen *et al.*⁴ still lacked a consistent description of this five-nucleon system, as for example the channels with $S = \frac{1}{2}$ and $\frac{3}{2}$ are described within a different model space. Furthermore, the NN interaction has been adjusted to the $n + \alpha$ phase shifts without considering other than the $n + \alpha$ configurations and, consequently, by neglecting the tensor component in the NN interaction. However, this component allows for a coupling of the $d + {}^3\text{He}$ channel with spin $S = \frac{3}{2}$ to the $p + \alpha$ channel as well as to the $d + {}^3\text{He}$ configuration with $S = \frac{1}{2}$. Such a coupling is particularly important for studying the properties of the $J^\pi = \frac{3}{2}^+$ resonance at $E_d = 245$ keV,⁵ which is known^{6,7} to dominate the ${}^3\text{He}(d,p){}^4\text{He}$ cross section at low energies ($E_p \leq 300$ keV). This state is mainly given by a $d + {}^3\text{He}$ configuration with orbital angular momentum $L = 0$ and with spin $S = \frac{3}{2}$, which in turn can only couple to the $p + \alpha$ channel via the tensor component in the NN interaction.^{7,8} Thus, it seems to be desirable to perform a microscopic study of the $d + {}^3\text{He}$ system which goes beyond the one reported in Ref. 4.

In this paper we want to report about a microscopic multichannel calculation performed in the framework of the resonating group method (RGM) in which we have

studied the ${}^5\text{Li}$ nucleus consistently within the same model space spanned by $p + \alpha$ and $d + {}^3\text{He}$ configurations as well as $d + {}^3\text{He}$ pseudostates and by using the same NN interaction containing a central, a spin-orbit, and a tensor component. From a formal point of view our study is a straightforward extension of the approaches reported in Refs. 3 and 4. Thus, we will restrict ourselves in Sec. II to outline only the basic theoretical ingredients of our calculation and refer the reader for further details and motivation to Refs. 3 and 4. In Sec. III, we then demonstrate that one is indeed able to simultaneously describe the low-energy $p + \alpha$ and $d + {}^3\text{He}$ systems, including the known levels in ${}^5\text{Li}$, within such a consistent theoretical approach.

II. THEORETICAL BACKGROUND

In our study of ${}^5\text{Li}$, the model space was spanned by $p + \alpha$ and $d + {}^3\text{He}$ configurations as well as by $d^* + {}^3\text{He}$ pseudostates in the sense of Ref. 4. Thus, the many-body wave function Ψ_J^π with total angular momentum J and parity π has been chosen to be

$$\begin{aligned} \Psi_J^i = & \mathcal{A} \{ [(\phi_\alpha^{I=0} \phi_p^{I=1/2})_{S=1/2}^{\pi=+} Y_L(\hat{r}_\alpha)]_J g_{JL}(r_\alpha) \} \\ & + \sum_{i=1}^3 \mathcal{A} \{ [(\phi_{d,i}^{I=1} \phi_{\text{He}}^{I=1/2})_{S=1/2}^{\pi=+} Y_L(\hat{r}_d)]_J h_{JL}^i(r_d) \} \\ & + \sum_{i=1}^3 \sum_{L'} \mathcal{A} \{ [(\phi_{d,i}^{I=1} \phi_{\text{He}}^{I=1/2})_{S=3/2}^{\pi=+} Y_{L'}(\hat{r}_d)]_J f_{JL'}^i(r_d) \} . \end{aligned} \quad (1)$$

Here, ϕ_α , ϕ_{He} , and $\phi_{d,i}$ describe the internal degrees of freedom of the α particle, the ${}^3\text{He}$ nucleus, the deuteron ground state ($i=1$), as well as of the deuteron pseudostates ($i=2,3$).

The explicit form of the wave functions will be discussed below. ϕ_p is the spin-isospin function of the proton. The internal spins of the fragments I are coupled to the channel spins S , which can take the value $S = \frac{1}{2}$ for the $p + \alpha$ system, while it can be $S = \frac{3}{2}, \frac{1}{2}$ for the $d + {}^3\text{He}$ system. The relative orbital angular momentum between the fragments L and the channel spin S are coupled to the total angular momentum J . Considering that all fragment wave functions have positive parity, the total parity

of the many-body wave function is determined by the parity of the relative wave function. Thus, for a given pair (J, π) we can only have one value for L in the $p + \alpha$ channel and in the $d + {}^3\text{He}$ channel with $S = \frac{1}{2}$, while in the $d + {}^3\text{He}$ channel with $S = \frac{3}{2}$ the orbital angular momentum might take two values between $L = J - \frac{1}{2}$ and $J + \frac{3}{2}$.

For the internal fragment wave functions we closely followed Refs. 3 and 4. For ϕ_α and ϕ_{He} we used

$$\phi_\alpha = \exp \left[-\frac{1}{2}\beta_4 \sum_{k=1}^4 \left(\mathbf{r}_k - \mathbf{R}_\alpha \right)^2 \right]; \quad \mathbf{R}_\alpha = \frac{1}{4} \sum_{k=1}^4 \mathbf{r}_k, \quad (2)$$

$$\phi_{\text{He}} = \exp \left[-\frac{1}{2}\beta_3 \sum_{k=1}^3 \left(\mathbf{r}_k - \mathbf{R}_{\text{He}} \right)^2 \right]; \quad \mathbf{R}_{\text{He}} = \frac{1}{3} \sum_{k=1}^3 \mathbf{r}_k. \quad (3)$$

For the choice of the deuteron ground state function $\phi_{d,1}$ and the excited pseudostates $\phi_{d,2}$ and $\phi_{d,3}$ we adopt the procedure from Shen *et al.*⁴ Thus, we start from a set of basis functions ($j = 1, \dots, 3$):

$$\chi_j(\alpha_j) = \exp \left[-\frac{1}{2}\alpha_j \sum_{k=1}^2 \left(\mathbf{r}_k - \mathbf{R}_d \right)^2 \right], \quad \mathbf{R}_d = \frac{1}{2} \sum_{k=1}^2 \mathbf{r}_k, \quad (4)$$

and determine the parameters α_j by minimizing the expectation value of the deuteron Hamiltonian in the space spanned by the basis functions χ_j . Our deuteron ground state wave function then reads

$$\phi_{d,1} = \sum_{j=1}^3 A_j^1 \chi_j(\alpha_j), \quad (5)$$

with the coefficients A_j^1 determined from the minimization procedure. The pseudostates are then obtained as the two excited levels found by diagonalization of the deuteron Hamiltonian in the space spanned by the χ_j , however, now keeping the parameters α_j fixed to the values determined for the deuteron ground state. Thus, ($i = 2, 3$).

$$\phi_{d,i} = \sum_{j=1}^3 A_j^i \chi_j(\alpha_j). \quad (6)$$

Note that these pseudostates do not correspond to realistic deuteron states. They might simply be understood as a tractable way to generate additional basis wave functions in the microscopic cluster model space which then allow us to take account of a possible distortion of the deuteron in the presence of other nucleons.

Our many-body Hamiltonian H reads as follows:

$$H = - \sum_{i=1}^5 \frac{p_i^2}{2m} + \sum_{i>j=1}^5 V_{ij} - T_{\text{c.m.}}, \quad (7)$$

where $T_{\text{c.m.}}$ is the kinetic-energy operator of the center-of-mass motion. Our NN interaction V_{ij} contains a central, a spin-orbit, and a tensor part which all have been parametrized to reproduce experimentally known properties of few-body bound and scattering states and have been used in previous studies of the five-nucleon system. In a first approach we adopted the NN interaction which

has been successfully applied to the studies of various few-nucleon systems by the Minnesota group. However, this potential consists only of a central part [Wildermuth-Tang (WT) force, Ref. 11] and a spin-orbit potential.⁹ In order to allow for a coupling of the $d + {}^3\text{He}$ channel with spin $S = \frac{3}{2}$ to the $p + \alpha$ channel, we completed the Minnesota NN interaction by the tensor potential of Ref. 10 which has been shown previously to give a quantitatively correct description of the coupling of the two channels if combined with the Minnesota potential.⁷ This first approach might be viewed as a direct extension of the one reported in Ref. 4. As it was *a priori* not known whether this study yields a correct description of the ${}^5\text{Li}$ level spectrum, we have performed in parallel another calculation in which the WT force in the NN interaction has been replaced by the Hasegawa-Nagata (HN) force¹² which has also been frequently used in successful studies of few-nucleon systems. In the present case, this second approach was particularly motivated by the results of Ref. 7 which showed that the low-energy ${}^3\text{He}(d,p){}^4\text{He}$ cross section can be quantitatively reproduced by this combination of the NN interaction. It is the usual custom in applications using the WT or HN interactions to adjust one parameter of this force (the exchange-mixture parameter u in case of the WT force and the Majorana parameter m_2 of the Gaussian component with medium range for the HN force) to selected experimental data. We will discuss our choice for u and m_2 in the next section. Note that the properties of the various fragments (deuteron, ${}^3\text{He}$, ${}^4\text{He}$) do not depend on u or m_2 .

For the WT force the parameters $\beta_3, \beta_4, \alpha_j$, and A_j^i are given in Ref. 4, where the parameter A_3^1 should read -0.1199 . Following the procedure outlined above we determined the deuteron ground state for the HN force as

$$\phi_{d,1} = 0.0924\chi_1(\alpha_1) + 1.752\chi_2(\alpha_2) - 1.537\chi_3(\alpha_3), \quad (8)$$

while the two pseudostates read

$$\phi_{d,2} = 0.1468\chi_1(\alpha_1) - 3.923\chi_2(\alpha_2) + 3.483\chi_3(\alpha_3); \quad (9)$$

$$\phi_{d,3} = 0.0502\chi_1(\alpha_1) - 8.927\chi_2(\alpha_2) + 10.213\chi_3(\alpha_3),$$

with the width parameters $\alpha_1 = 0.12 \text{ fm}^{-2}$, $\alpha_2 = 1.2 \text{ fm}^{-2}$, and $\alpha_3 = 1.4 \text{ fm}^{-2}$. With this parametrization, the deuteron in the ground state has a binding energy of 2.32 MeV, while the pseudostates are at excitation energies of $E_x = 15.61 \text{ MeV}$ and 149.86 MeV , respectively. The parameters β_3 and β_4 for the HN force are given in Ref. 13.

Following the standard procedure,⁸ the unknown relative wave functions g, h , and f are determined by solving the many-body Schrödinger equation in the space spanned by the internal $d + {}^3\text{He}$ and $p + \alpha$ basis wave functions. This leads to the well known RGM set of coupled integrodifferential equations⁸ which we have solved by a discretization method using 60 meshpoints with equidistant spacing of 0.3 fm for each relative coordinates in the various channels and by imposing the usual boundary conditions for scattering states. This procedure turned out to be accurate enough as at all investigated energies

the calculated S matrix was found to be unitary and symmetric which is not *a priori* built into our numerical solution of the RGM equations.

III. RESULTS AND DISCUSSION

With respect to the compilation of Ajzenberg-Selove¹⁴ the following states in ${}^5\text{Li}$ are known experimentally: the ${}^5\text{Li}$ ground state ($J^\pi = \frac{3}{2}^-$) at an energy $E_p \approx 1.96$ MeV above the $p + \alpha$ threshold, a very broad $\frac{1}{2}^-$ state at an energy of $E_p \approx 7-12$ MeV, and the narrow $\frac{3}{2}^+$ resonance at $E_d = 0.245$ MeV just above the $d + {}^3\text{He}$ threshold. The compilation also lists possible states at $E_d = 1.6$ MeV ($J^\pi = \frac{1}{2}^+$) and at $E_d \approx 3.4$ MeV ($J^\pi = \frac{5}{2}^+$ or $\frac{3}{2}^+$), which, however, are not uniquely verified yet (for references see Ref. 14).

In this section we want to study these ${}^5\text{Li}$ levels consistently within the theoretical model outlined in Sec. II. The values of the exchange-mixture parameter u in the WT force and the Majorana parameter m_2 in the HN force were adjusted to the energy position of the $\frac{3}{2}^+$ resonance at $E_d = 245$ keV. From this requirement we obtained $u = 0.835$ and $m_2 = 0.41$. As we will demonstrate in the following we are able to reproduce the experimentally known levels in ${}^5\text{Li}$ consistently in our first approach using the WT force without adjustment of any further parameter. However, this is not the case in the approach based on the Hasegawa-Nagata force which, as we will show below, is inferior to the WT force in the description of the ${}^5\text{Li}$ spectrum. Additionally, in this approach we had to change the strength of the tensor force slightly in order to reproduce the magnitude of the resonant ${}^3\text{He}(d,p){}^4\text{He}$ cross section. Thus, in our calculations using the HN force we used the parameter $V_T^1 = -85.94$ MeV in the tensor component of the NN interaction, while we adopted the original parametrization for this force ($V_T^1 = -100.94$ MeV, Ref. 10) in our studies based on the WT force. Note that we additionally modified the strength of the spin-orbit force in our calculation based on the HN interaction (here we used $V_{LS} = -205$ MeV) in order to reproduce the splitting in the $p + \alpha$ p -wave phase shifts.

The quality of the description for the p -wave states in ${}^5\text{Li}$ can be tested by comparison of the calculated $p + \alpha$ phase shifts with the “experimental” ones of Ref. 15 and the “empirical” phase shifts of Ref. 16. For the $\frac{3}{2}^+$ resonance a stringent test between theory and experiment is given by comparing the ${}^3\text{He}(d,p){}^4\text{He}$ fusion cross section which at low energies is dominated by this state.⁷

Before we compare our results with experimental data, we would like to mention that our calculation exhibits one shortcoming which is implicit to all cluster approaches of the $d + {}^3\text{He}$ and $p + \alpha$ systems using the WT or HN forces. Although these NN interactions give a fair account of the properties of the various fragments, they overestimate the $d + {}^3\text{He}$ threshold with respect to the $p + \alpha$ threshold by about 1.8 MeV. Note that the $J^\pi = \frac{3}{2}^+$ state mainly corresponds to a state formed in the $d + {}^3\text{He}$ channel with $L = 0$ and $S = \frac{3}{2}$ at an energy below the Coulomb barrier and is therefore rather sensitively dependent on penetration effects. For a meaningful study

of this state it is therefore reasonable and standard^{3,4,7,10} to measure energies relatively to the $d + {}^3\text{He}$ threshold. However, the slight overestimation of the $p + \alpha$ and $d + {}^3\text{He}$ channel splitting (experimental value $Q = 18.35$ MeV) leads to some inconsistency when comparing theoretical results to experimental data at energies above the $d + {}^3\text{He}$ threshold. For this reason we will not discuss the $p + \alpha$ phase shifts at energies above the $d + {}^3\text{He}$ threshold. Furthermore, we will restrict the present study of the ${}^5\text{Li}$ nucleus to excitation energies below ≈ 20 MeV, as at higher energies other than the presently considered, fragmentations (i.e., three-body breakup channels) may become important.

The $p + \alpha$ phase shifts are shown in Fig. 1. At energies around the two ${}^5\text{Li}$ p -wave resonances, the WT force reproduces the experimental phase shifts very well suggesting that this approach gives a good description of these states. However, the agreement is somewhat worse at higher energies, where the calculated phase shifts are lower than the experimental ones by a few degrees. The HN interaction overbinds these two ${}^5\text{Li}$ states slightly resulting in an overestimation of the phase shifts in the energy regime $E_p \leq 16$ MeV. In the $s_{1/2}$ partial wave both forces slightly overestimate the experimental phase shifts.

The low-energy ${}^3\text{He}(d,p){}^4\text{He}$ cross sections are most conveniently studied in terms of the astrophysical S factor

$$S(E_d) = E_d \sigma(E_d) \exp[2\pi\eta(E_d)], \quad (10)$$

where the Sommerfeld parameter η is defined by $2\pi\eta(E_d) = 2.1737/\sqrt{E_d}$ with the energy in the $d + {}^3\text{He}$ channel measured in MeV.

In Fig. 2 our calculated results are compared with the experimental data of Refs. 6 and 17. For both interactions we find an excellent agreement to the data of Krauss *et al.*⁶ in the range $E_d > 30$ keV. At lower energies, the S factors calculated for the WT and HN forces are nearly identical, but they both are smaller than the experimental data. However, as we will discuss below, the experimental cross sections are enhanced due to electron screening effects (see below and Refs. 7, 18, and 19). Considering the estimated errors of $\leq 6\%$ in the data of Besenbacher and Möller¹⁷ our results are also in good agreement with this data set. Note that there is an additional 6% uncertainty in the overall normalization factor of the two experimental data sets.²⁰

As the low-energy ${}^3\text{He}(d,p){}^4\text{He}$ cross section is strongly dominated by the $\frac{3}{2}^+$ resonance at about $E_d = 245$ keV, the good agreement between experiment and theory (Fig. 2) indicates that our theoretical approach is able to reproduce this excited ${}^5\text{Li}$ level. This might again be tested by inspecting the $p + \alpha$ phase shift in the $d_{3/2}$ partial wave, which is the only one in the $p + \alpha$ channel which can couple to the $J^\pi = \frac{3}{2}^+$ resonance. In Fig. 3 we compare the calculated $d_{3/2}$ phase shifts with the experimental values of Refs. 21 and 22 and the very recent ones of Burzynski *et al.*²³ Although our calculation reproduces the trend of the phase shifts, including the resonant part, for both interactions the calculated phase shifts are systematically by a few degrees lower than the data of Plattner *et al.*²¹ and of Houdayer *et al.*²² This might indicate that our

theoretical approach estimates too weak a $p + \alpha$ contribution. However, our phase shifts agree better with the recent analysis of Burzynski *et al.*²³ Note that these authors have pointed out that the solution of Ref. 21 in the $d_{3/2}$ partial wave was fixed by results from an R -matrix calculation which restricted the flexibility of the fit in Ref. 21 and resulted in the uncertainties between the experimental phase shift sets of Refs. 21 and 22 and of Ref. 23 as shown in Fig. 3. It would be interesting to see how much this restricted flexibility affects the phase shifts in the vicinity of the $\frac{3}{2}^+$ resonance and how phase shifts analyzed along the lines of Ref. 23 compare with our calculated values in this energy regime.

In agreement with the experimental phase shift analyses^{21,22} as well as with previous microscopic calculations,^{4,10} neither of our calculations give evidence for a

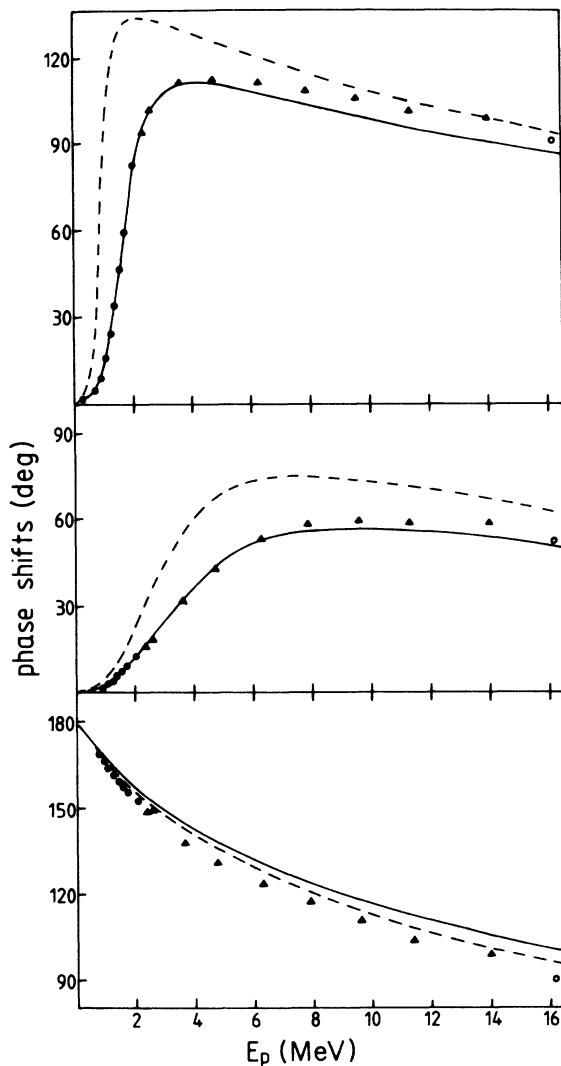


FIG. 1. Comparison of the $p + \alpha$ phase shifts calculated with the WT force (solid lines) and the HN force (dashed lines) with the experimental data of Refs. 15 and 22 (triangles and open circles, respectively) and the empirical data of Ref. 16 (dots).

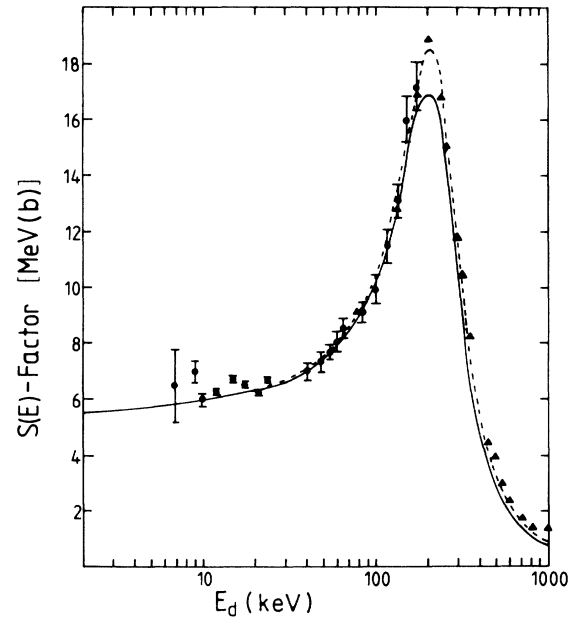


FIG. 2. Comparison of the ${}^3\text{He}(d,p){}^4\text{He}$ cross section calculated with the WT force (solid line) and the HN force (dashed line) with the experimental data of Refs. 6 and 17 (dots and triangles, respectively).

resonant state in ${}^5\text{Li}$ with $J^\pi = \frac{1}{2}^+$ at $E_d \approx 1-3$ MeV as hypothetically suggested to empirically explain measurements of the tensor analyzing powers in the low-energy ${}^3\text{He}(d,p){}^4\text{He}$ reaction.²⁴ We would like to mention that these measurements can be well reproduced on the basis of the present calculation.²⁵

In Fig. 4 we compare the $d + {}^3\text{He}$ phase shifts calculated with the WT force with the experimental values of Jenny *et al.*²⁷ Considering the scatter of the different phase shift solutions given in Ref. 27, the agreement in the $S = \frac{3}{2}$ partial waves is good including the energy regime dominated by the $\frac{3}{2}^+$ resonance. The agreement is worse for the phase shifts in the $S = \frac{1}{2}$ channels where we seem to underestimate the experimental values. Our calculated phase shifts are similar to those obtained in previous microscopic multichannel calculations^{4,10} except for the s -wave phase shift in the $S = \frac{3}{2}$ channel where we obtain a better agreement to the experimental values due to the correct reproduction of the resonance energy. Similar to the results of Ref. 4 and the phase shift analysis of Jenny *et al.*,²⁷ we find broad resonance-like structures in all d -wave phase shifts of the $d + {}^3\text{He}$ system with the fragment spins coupled to $S = \frac{3}{2}$. In particular, we observe for both effective NN interactions a broad resonant $\frac{5}{2}^+$ structure at energies around $E_d \approx 4$ MeV which might correspond to the state tentatively included in the compilation of Aizenberg-Selove.¹⁴

How do the present results compare with those of Tang and collaborators^{1,4} who have performed their studies of ${}^5\text{Li}$ using the WT interaction? At first, we find that the inclusion of a $d + {}^3\text{He}$ configuration has a sizable

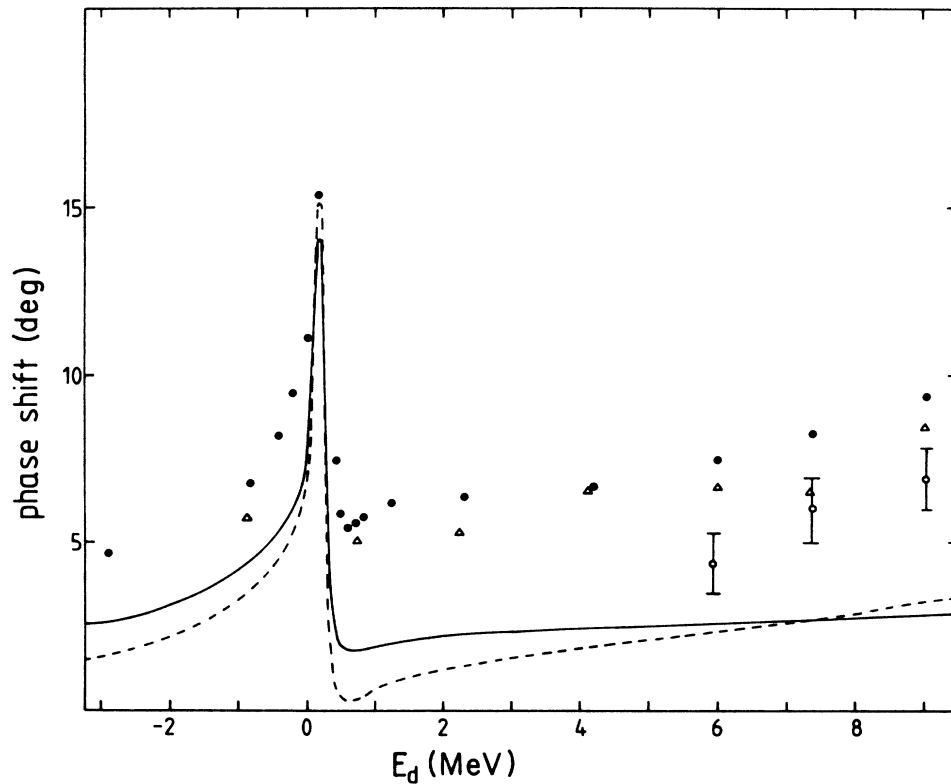


FIG. 3. Comparison of the $p + \alpha$ phase shifts in the $d_{3/2}$ partial wave calculated with the WT force (solid line) and the HN force (dashed line) with the experimental data of Plattner *et al.* (Ref. 21) (full circles), Houdayer *et al.* (Ref. 22) (triangles), and Burzynski *et al.* (Ref. 23).

effect on the $p + \alpha$ phase shifts, even at energies at which the $d + {}^3\text{He}$ channel is closed. The strongest effects are observed in the $p_{3/2}$ and $p_{1/2}$ partial waves in the range of the respective resonances. To be more quantitative, in a study based on a single $p + \alpha$ configuration, Chwieroth, Thompson, and Tang³ obtained a reproduction of the

$p + \alpha$ phase shifts using a value for the exchange-mixture parameter $u = 0.95$ rather than the present $u = 0.835$. We find that both the inclusion of the $d + {}^3\text{He}$ configuration and that of the tensor component in the NN interaction contribute to these observed differences. Thus, our calculation seems to indicate that the two

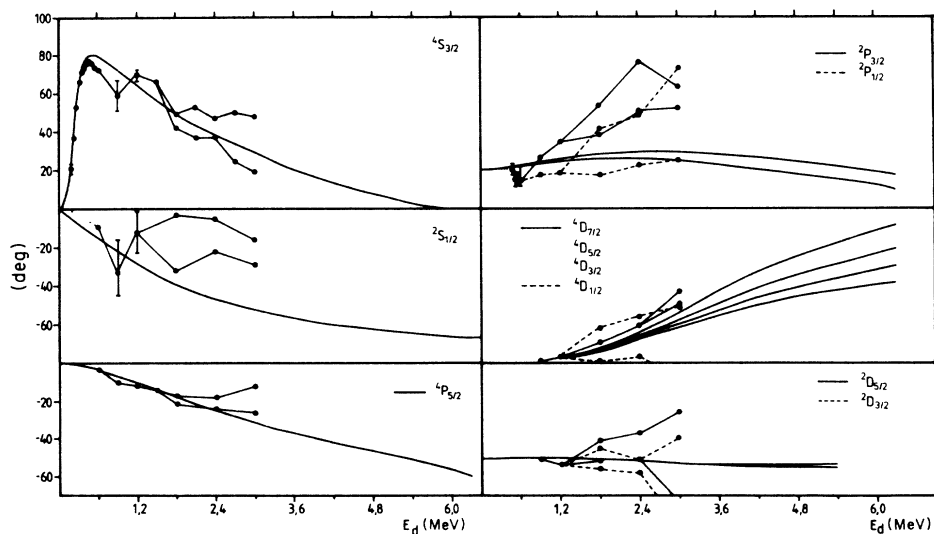


FIG. 4. Comparison of the $d + {}^3\text{He}$ phase shifts calculated with the Minnesota force (solid lines) with the experimental ones analyzed by Jenny *et al.* (Ref. 27). The theoretical phase shifts are ordered in the same sequence as the partial wave symbols given. The full and open dots refer to the solutions $G1$ and $G2$ as defined in Ref. 27. To guide the eye, the experimental phase shifts belonging to the different solutions are connected by lines. The correspondence of the lines to the various partial waves is indicated in front of the partial wave symbols.

lowest ${}^5\text{Li}$ levels are not of pure $p + \alpha$ configuration, although the latter still dominates the structure of these states. However, such an interpretation can be somewhat misleading as the origin of this effect might be in the fact that the presently chosen ${}^4\text{He}$ wave function is not variationally stable with respect to cluster formation. Tang and collaborators found such a behavior in a study of the four-nucleon system, however, adopting a different effective NN interaction.²⁶ Hence, the added freedom of $d + {}^3\text{He}$ configurations can add some degree of $p + {}^3\text{H}$ or $n + {}^3\text{H}$ structure into the ${}^4\text{He}$ wave function which improves this latter one, but does then not indicate the necessity of a $d + {}^3\text{He}$ component in the ${}^5\text{Li}$ ground state. The distortion effects become less important at off-resonant energies. In the $s_{1/2}$ partial wave our calculation yields a slightly worse reproduction of the experimental phase shifts than the single-channel study of Ref. 3. Thus, our approach might overestimate distortion effects in this partial wave.

As outlined above, the $\frac{3}{2}^+$ resonance, formed mainly in the $d + {}^3\text{He}$ channel with spin $S = \frac{3}{2}$, can only weakly couple to $S = \frac{1}{2}$ configurations via the tensor component in the NN interaction. Thus, our extended model space does not significantly alter the results obtained for this state by Shen *et al.*⁴ in their study based on a $d + {}^3\text{He}$ configuration and on $d^* + {}^3\text{He}$ pseudostates with $S = \frac{3}{2}$. For example, using the value $u = 0.95$ as in Ref. 4, we find the resonance shifted towards lower energies by about 100 keV due to coupling to $S = \frac{1}{2}$ configurations in our enlarged model space. This has to be compared to an energy shift of about 360 keV mediated by distortion effects due to the two $d + {}^3\text{He}$ pseudostates already discussed by Shen *et al.*⁴ Nevertheless, our calculation allows us for the first time to quantitatively study the coupling to the $p + \alpha$ channel, a quantity which has been experimentally explored by measuring the reaction cross section in the resonant regime.

As mentioned above, the experimental ${}^3\text{He}(d,p){}^4\text{He}$ cross sections at $E_d \leq 30$ keV are noticeably higher than (i) those calculated in the present approach (see Fig. 2) and (ii) as expected from the extrapolated energy dependence of the measured cross section at higher energies.¹⁹ This behavior has been associated with an electron screening effect¹⁸ caused by the presence of electrons in the atomic ${}^3\text{He}$ target gas. Although the evidence for the existence of this effect in the data of Ref. 19 is quite convincing, a quantitative analysis of the electronic screening strength requires a precise knowledge of the pure nuclear cross section at low energies. Based on a microscopic study of the ${}^3\text{He}(d,p){}^4\text{He}$ reaction using only $p + \alpha$ and $d + {}^3\text{He}$ configurations it was concluded that the low-energy ${}^3\text{He}(d,p){}^4\text{He}$ cross section is entirely given by the resonant contribution arising from the $\frac{3}{2}^+$ resonance.⁷ Consequently the low-energy ${}^3\text{He}(d,p){}^4\text{He}$ cross section has been determined in Ref. 7 by a Breit-Wigner fit to the experimental data at $E_d > 40$ keV which are free of electron screening effects. Discussing the enhancement of the measured low-energy cross sections over the obtained Breit-Wigner fit led to the noticeable result that the electron screening effects could not be described by models

based on a Born-Oppenheimer-type approximation.⁷

The findings presented in Ref. 7 are not quite supported by the results of our present approach which indicates that the ${}^3\text{He}(d,p){}^4\text{He}$ cross section at very low energy ($E_d < 20$ keV) is still dominated by the contribution arising from the $\frac{3}{2}^+$ resonance, but, in contrast to Ref. 7, contributions due to the interference of the resonance with background terms cannot quite be neglected. As our calculation predicts this interference to be constructive, the presently calculated cross section at $E_d < 20$ keV is somewhat larger than the one obtained in Ref. 7. Note that this is also partly due to the fact that we have here used the experimental masses in calculating the Sommerfeld parameter rather than the pure nucleonic mass numbers as in Ref. 7.

Our approach predicts a ${}^3\text{He}(d,p){}^4\text{He}$ S factor which, with decreasing energy, increasingly exceeds the Breit-Wigner fit to the low-energy ${}^3\text{He}(d,p){}^4\text{He}$ cross section presented in Ref. 7. Vice versa, adopting the present S factor rather than the Breit-Wigner fit predicts weaker electron screening effects than deduced in Ref. 7. To be quantitative, the present S factor is larger by about 7% than the recommendation of Ref. 7 at $E_d = 5.88$ keV which is the lowest energy at which the ${}^3\text{He}(d,p){}^4\text{He}$ cross section has been measured in Ref. 19. The corresponding reduction in the electron screening effects seems to bring the latter in marginal agreement with the predictions of the Thomas-Fermi model (see Fig. 5 of Ref. 7). We are planning to reanalyze the data of Ref. 19 for electron screening effects using the presently calculated low-energy S factor as an estimate for the pure nuclear S factor.

In conclusion, we have studied the spectrum of ${}^5\text{Li}$ consistently within a multichannel approach based (i) on microscopic $\alpha + p$ and $d + {}^3\text{He}$ cluster configurations as well as on $d^* + {}^3\text{He}$ pseudostates in the sense of Ref. 4 and (ii) on an effective NN interaction containing a central, a spin-orbit, and a tensor component. It should be noted that in an approach in which we used the Minnesota potential supplemented by a tensor component from the literature, we exactly reproduced the energy positions and widths of the three lowest resonances in ${}^5\text{Li}$ after the usual adjustment of a single parameter in the central part of the interaction. This is an advantageous result as it will allow us to calculate for the first time the γ width of the $\frac{3}{2}^+$ resonance which decays mainly by $E1$ transition into the ${}^5\text{Li}$ ground state. Such a calculation is in progress. The description of the ${}^5\text{Li}$ spectrum was worse in a calculation in which we used the Hasegawa-Nagata force as the central component of the NN interaction, although the low-energy ${}^3\text{He}(d,p){}^4\text{He}$ cross section was well reproduced in this approach.

We expect that an approach similar to the present one will also give a good description of ${}^5\text{He}$, the analog nucleus of ${}^5\text{Li}$. Such a calculation is in progress. Provided its success, one is then able to calculate for the first time the γ - and particle-decay widths of the $\frac{3}{2}^+$ resonance just above the $\alpha + n$ threshold. These quantities are of vital interest for the analysis of hot plasmas in nuclear fusion reactors.

- ¹Y. Fujiwara, Q. K. K. Liu, and Y. C. Tang, Phys. Rev. C **38**, 1531 (1988).
- ²H. Kanada, T. Kaneko, and Y. C. Tang, Phys. Rev. C **38**, 2013 (1988).
- ³F. S. Chwieroth, Y. C. Tang, and D. R. Thompson, Phys. Rev. C **9**, 56 (1974).
- ⁴P. N. Shen, Y. C. Tang, Y. Fujiwara, and H. Kanada, Phys. Rev. C **31**, 2001 (1985).
- ⁵Throughout this paper we refer to energies in the c.m. system. The index indicates with respect to which threshold (d for $d + {}^3\text{He}$, p for $p + \alpha$) the energies are measured.
- ⁶A. Krauss, H. W. Becker, H. P. Trautvetter, C. Rolfs, and K. Brand, Nucl. Phys. **A465**, 150 (1987).
- ⁷G. Blüge, K. Langanke, H. G. Reusch, and C. Rolfs, Z. Phys. **A 333**, 219 (1989).
- ⁸K. Wildermuth and Y. C. Tang, *A Unified Theory of the Nucleus* (Vieweg, Braunschweig, 1977).
- ⁹I. Reichstein and Y. C. Tang, Nucl. Phys. **A158**, 529 (1970).
- ¹⁰P. Heiss and H. H. Hackenbroich, Phys. Lett. **30B**, 373 (1969).
- ¹¹F. S. Chwieroth, R. E. Brown, Y. C. Tang, and D. R. Thompson, Phys. Rev. C **8**, 938 (1973).
- ¹²H. Furutani, H. Kanada, T. Kaneko, and S. Nagata, Prog. Theor. Phys. Suppl. **68**, 215 (1980).
- ¹³T. Kajino, Nucl. Phys. **A460**, 559 (1986).
- ¹⁴F. Ajzenberg-Selove, Nucl. Phys. **A490**, 1 (1988).
- ¹⁵P. Schwandt, T. B. Clegg, and W. Haeblerli, Nucl. Phys. **A163**, 432 (1971).
- ¹⁶L. Brown, W. Haeblerli, and W. Trächslin, Nucl. Phys. **A90**, 339 (1967).
- ¹⁷W. Möller and F. Besenbacher, Nucl. Instrum. Methods **168**, 111 (1980).
- ¹⁸H. J. Assenbaum, K. Langanke, and C. Rolfs, Z. Phys. **A 327**, 461 (1987).
- ¹⁹S. Engstler, A. Krauss, K. Neldner, C. Rolfs, U. Schröder, and K. Langanke, Phys. Lett. **B 202**, 179 (1988).
- ²⁰A. Krauss, Doctoral dissertation, Universität Münster, 1986.
- ²¹G. R. Plattner, A. D. Bacher, and H. E. Conzett, Phys. Rev. C **5**, 1158 (1972).
- ²²A. Houdayer, N. E. Davison, S. A. Elbakr, A. M. Sourkes, W. T. H. van Oers, and A. D. Bacher, Phys. Rev. C **18**, 1985 (1978).
- ²³S. Burzynski, J. Campbell, M. Hammans, R. Henneck, W. Lorenzon, M. A. Pickar, and I. Sick, Phys. Rev. C **39**, 56 (1989).
- ²⁴L. C. McIntyre and W. Haeblerli, Nucl. Phys. **A91**, 369 (1967).
- ²⁵G. Blüge, K. Langanke, M. Plagge, G. Nyga, and H. Paetzgen. Schieck, Phys. Lett. **B** (to be published).
- ²⁶H. Kanada, T. Kaneko, and Y. C. Tang, Phys. Rev. C **34**, 22 (1986).
- ²⁷B. Jenny, W. Gruebler, P. A. Schmelzbach, V. König, and H. R. Bürgi, Nucl. Phys. **A337**, 77 (1980).